

Supporting Information

Superelastic, highly conductive, and superhydrophobic silver nanowires@polypyrrole hybrid aerogels with outstanding electromagnetic interference shielding and Joule heating performance

Fei Peng^{a, b, 1}, Wenbo Zhu^{a, b, 1,*}, Bicheng Fu^a, Yi Fang^a, Zhipeng Peng^a, Jingjing He^a, Hongtao Chen^a,
Hongjun Ji^a, Chunjin Hang^b, Mingyu Li^{a, b,*}

^a Sauvage Laboratory for Smart Materials, School of Materials Science and Engineering, Harbin Institute of Technology (Shenzhen), Shenzhen, 518055, China

^b State Key Laboratory of Advanced Welding and Joining, Harbin Institute of Technology, Harbin, 150001, China

* Corresponding author.

E-mail address: zhuwenbo@hit.edu.cn

* Corresponding author.

E-mail address: myli@hit.edu.cn.

¹ Authors (Fei Peng and Wenbo Zhu) contributed equally to this work and should be considered co-first authors.

1. The EMI shielding performance of the AgNW@PPy hybrid aerogels

The power coefficients and EMI SE were calculated from scattering parameters (S_{11} and S_{21}) by the following formulas:

$$T = |S_{21}|^2 \quad (\text{S1})$$

$$R = |S_{11}|^2 \quad (\text{S2})$$

$$A = 1 - T - R \quad (\text{S3})$$

$$\text{SE}_T = -10\log(T) \quad (\text{S4})$$

$$\text{SE}_R = -10\log(1-R) \quad (\text{S5})$$

$$\text{SE}_A = \text{SE}_T - \text{SE}_R \quad (\text{S6})$$

where T , R , and A represent the transmissivity, reflectivity, and absorptivity, respectively. The SE_T , SE_R , and SE_A are the total, reflective, and absorptive values of EMI shielding effectiveness, respectively.

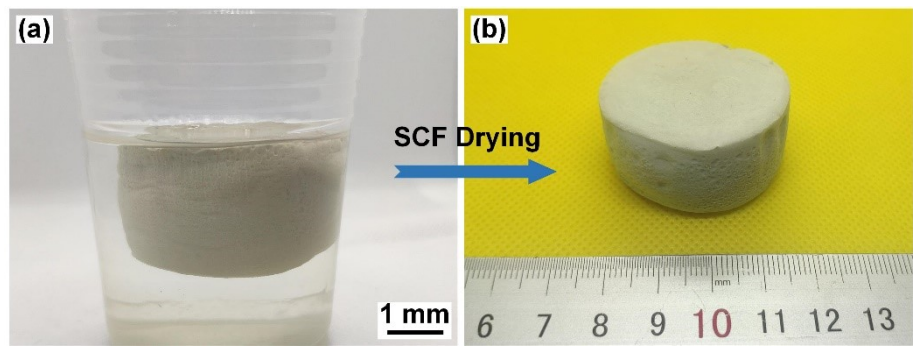


Fig. S1. Morphology of the (a) AgNW wet gel; (b) AgNW aerogel.

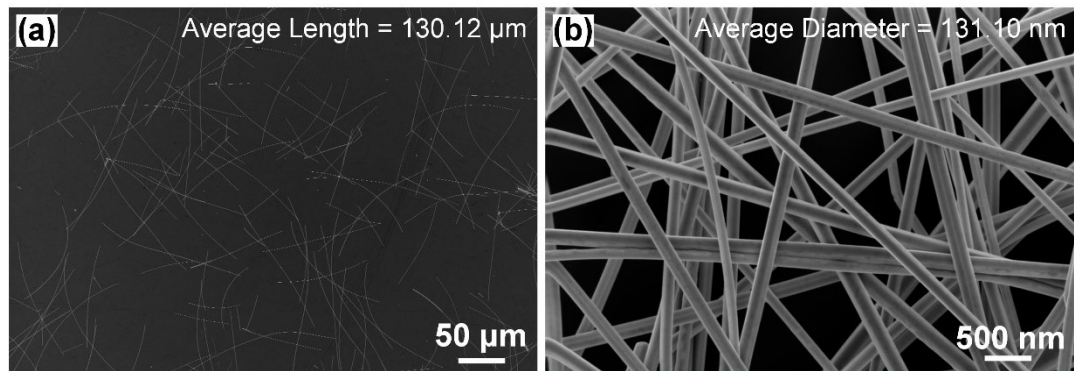


Fig. S2. SEM images of AgNWs which are taken down from the aerogel: (a) low-magnification image shows the length of the AgNWs; (b) high-magnification image shows the diameter of the AgNWs.

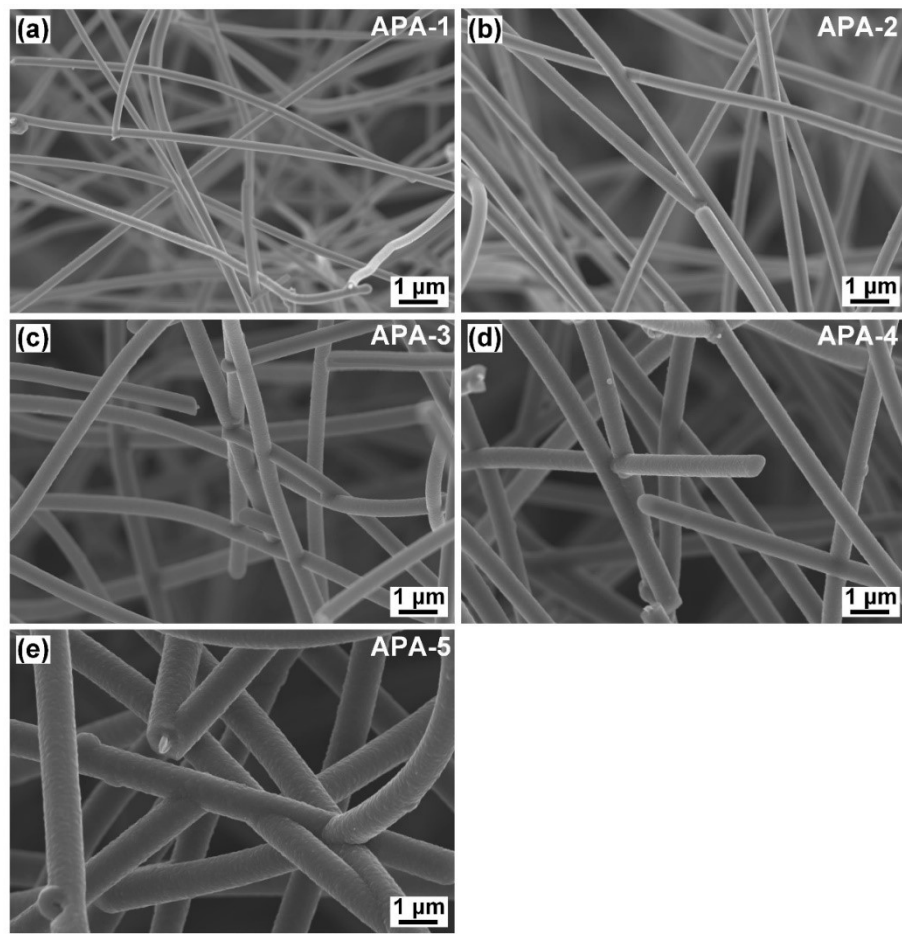


Fig. S3. SEM images of AgNW@PPy core-shell hybrid aerogel with different concentrations of pyrrole: (a) 3 mg L⁻¹; (b) 5 mg L⁻¹; (c) 8 mg L⁻¹; (d) 10 mg L⁻¹; (e) 15 mg L⁻¹.

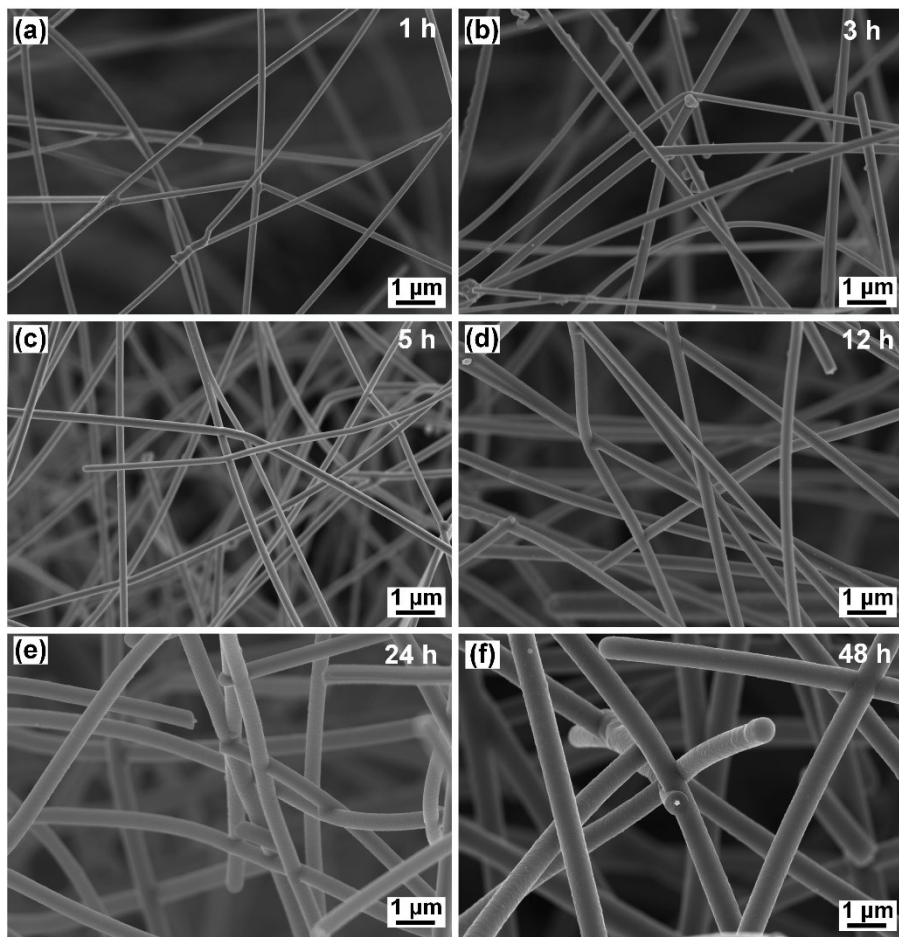


Fig. S4. SEM images of AgNW@PPy core-shell hybrid aerogel with different reaction times: (a) 1 h; (b) 3 h; (c) 5 h; (d) 12 h; (e) 24 h; (f) 48 h.

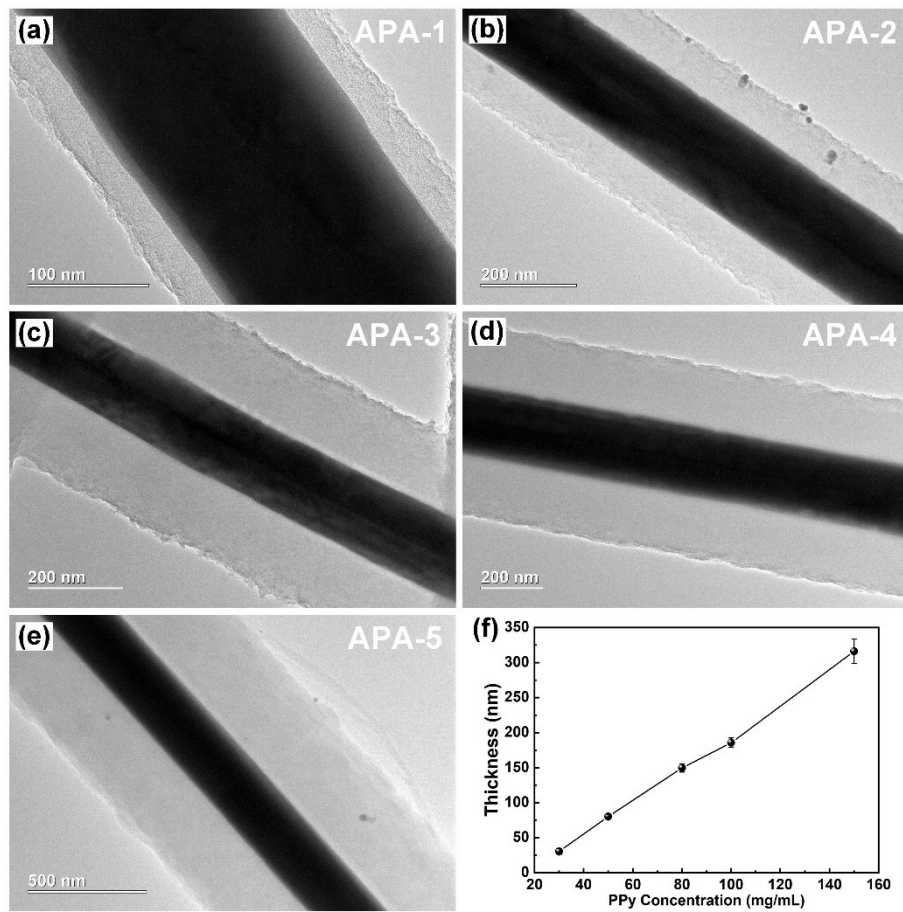


Fig. S5. TEM images of AgNW@PPy core-shell hybrid aerogel with different concentrations of pyrrole: (a) 3 mg L⁻¹; (b) 5 mg L⁻¹; (c) 8 mg L⁻¹; (d) 10 mg L⁻¹; (e) 15 mg L⁻¹ and (f) the relationship between the thickness of PPy layer and pyrrole concentration.

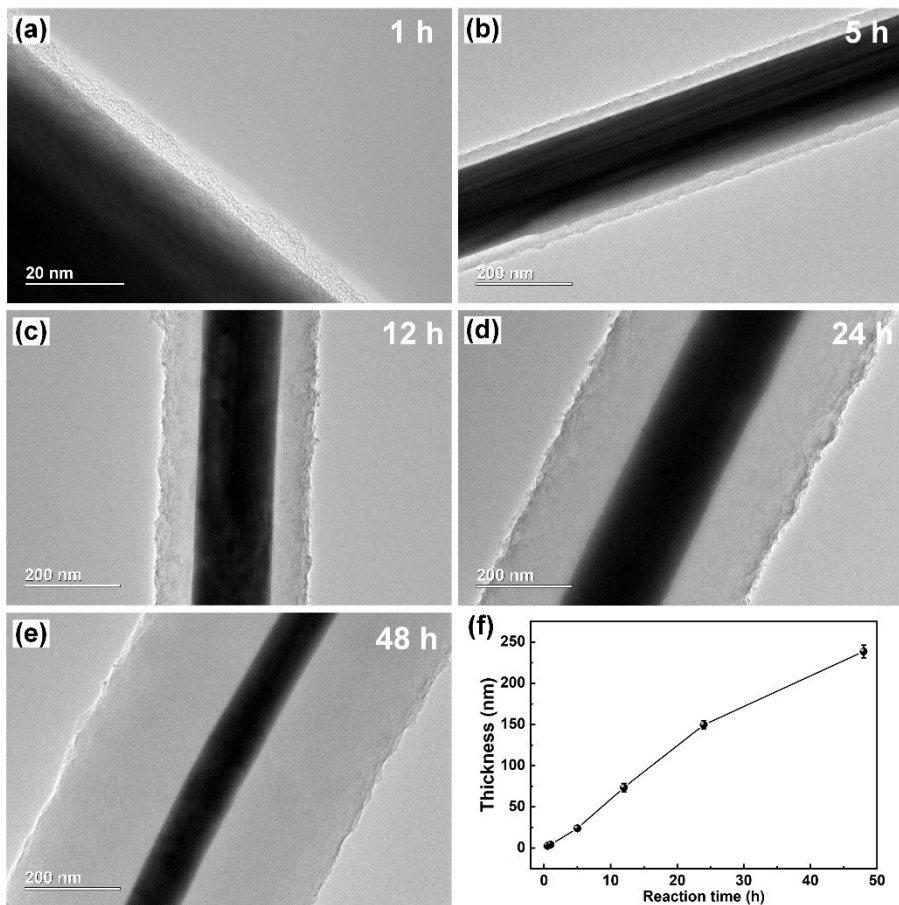


Fig. S6. TEM images of AgNW@PPy core-shell hybrid aerogel with different reaction times: (a) 1 h; (b) 5 h; (c) 12 h; (d) 24 h; (e) 48 h and (f) the relationship between the thickness of PPy layer and reaction time.

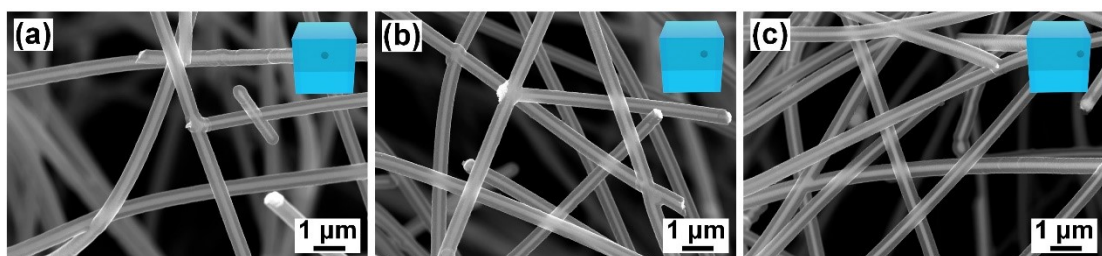


Fig. S7. PPy coating at different distances from the core of the sample: (a) 0 mm; (b) 2.5mm; (c) 5 mm.

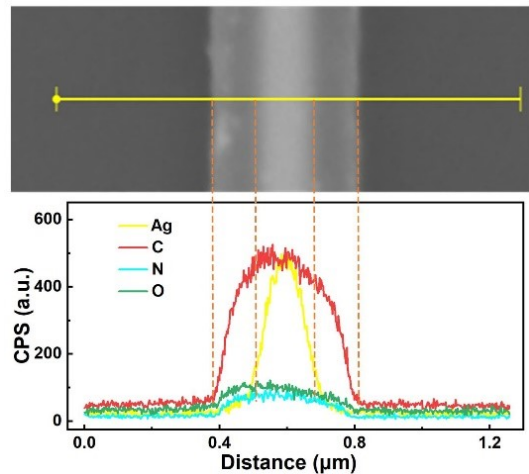


Fig. S8. Elemental distribution of the AgNW@PPy core-shell cable.

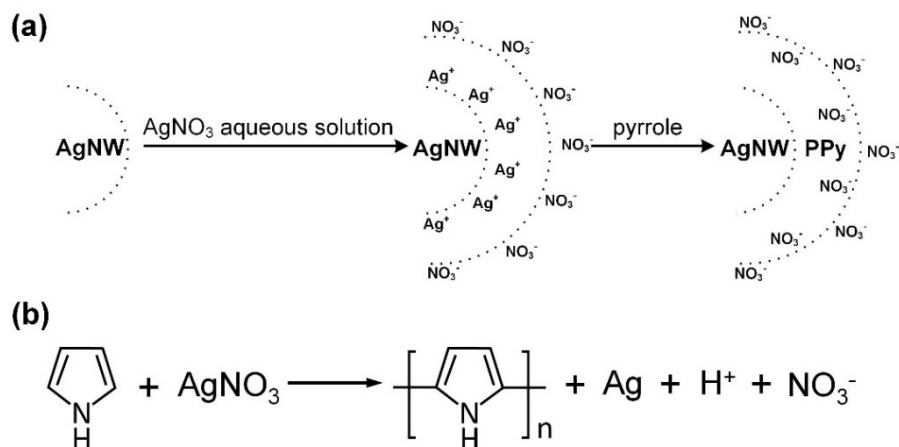


Fig. S9. Schematic formation mechanism of the AgNW@PPy nanocables through common ions adsorption effect.

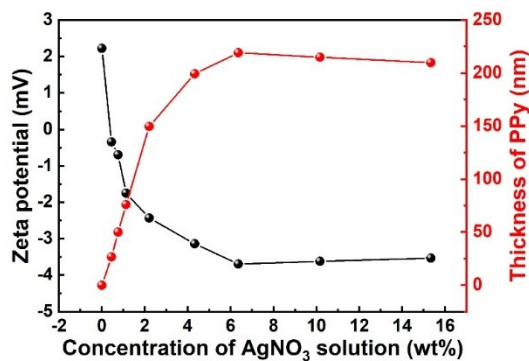


Fig. S10. Relationship between the zeta potential of AgNWs, the thickness of PPy layer, and the concentration of AgNO₃ aqueous solution.

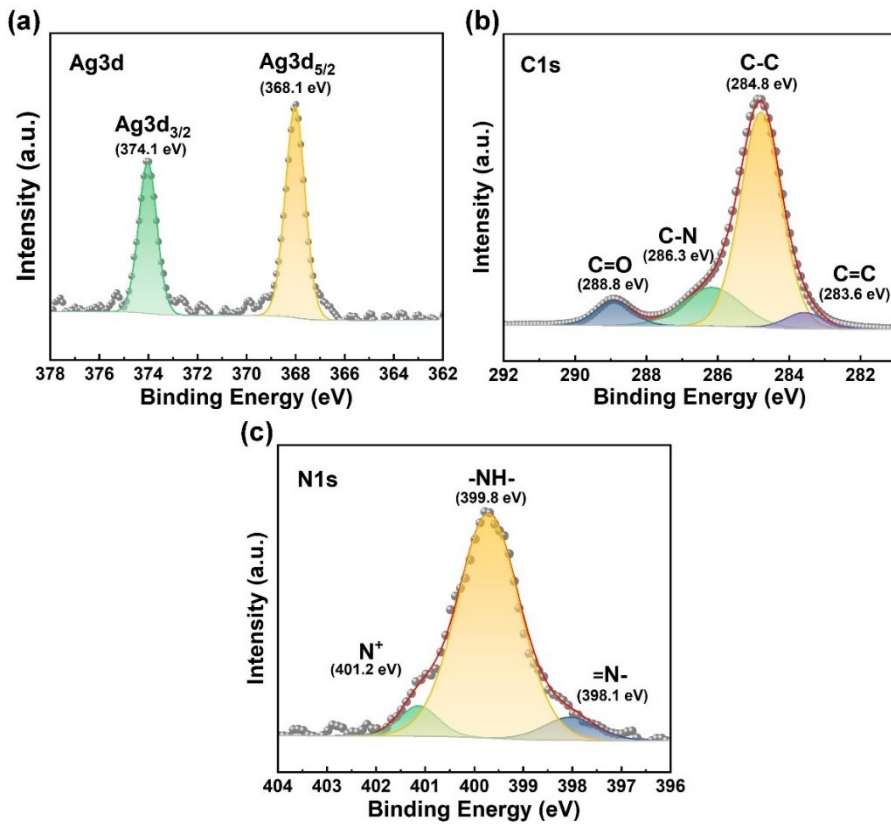


Fig. S11. XPS spectra of (a) Ag, (b) C, and (b) N of AgNW@PPy hybrid aerogel. Two peaks at 368.1 eV and 374.1 eV correspond to Ag 3d_{5/2} and Ag 3d_{3/2}, respectively, with a spin energy separation of 6.0 eV, which agrees with the reported value for elemental Ag0. The prominent peak at 284.8 eV is attributed to the C-C bond in the PPy backbone, while the binding energies at 283.6 eV and 286.3 eV are ascribed to the C=C and C-N bonding, respectively. The C=O bond energy is observed at 288.8 eV, which is due to the oxidation of carbon during the oxidative reaction in the PPy synthesis process. The N1s spectra can be divided into three components: a peak at 398.1 eV is corresponding to $=\text{N}-$, a peak at 399.8 eV is the characteristic peak of $-\text{NH}-$, a peak at 401.2 eV is attributed to $\text{C}-\text{N}^+$ and $-\text{C}=\text{N}^+$.

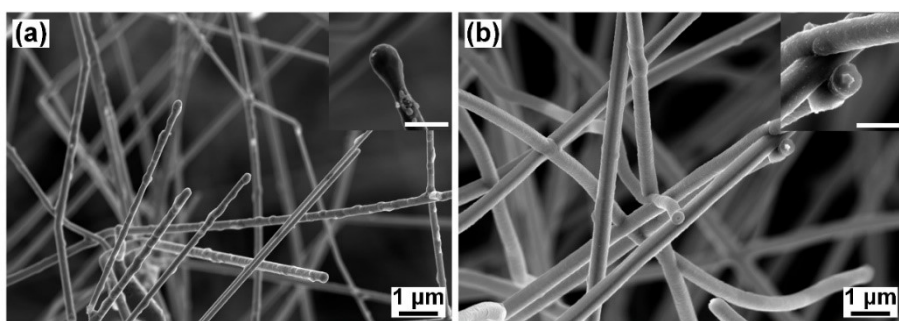


Fig. S12. Microstructure evolution of (a) AgNW aerogel and (b) AgNW@PPy hybrid aerogel after long-term stability test at 85 °C and 85 % RH for 28 days. The scale bar in the inset is 500 nm.

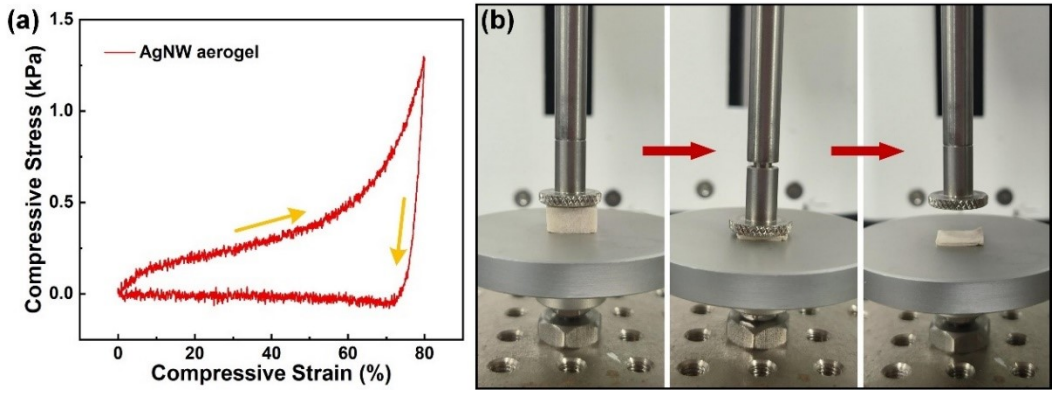


Fig. S13. (a) Compressive stress-strain curves of AgNW aerogel; (b) a set of digital images show the unrecoverable performance of AgNW aerogel.

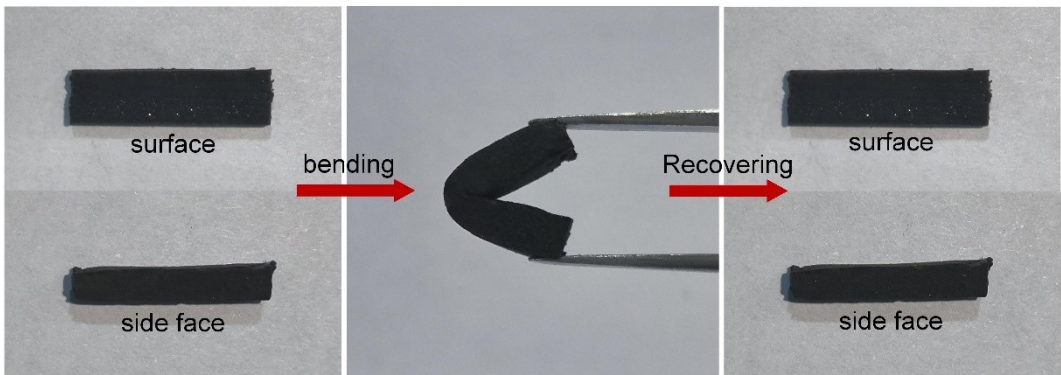


Fig. S14. The bending property of AgNW@PPy hybrid aerogel.

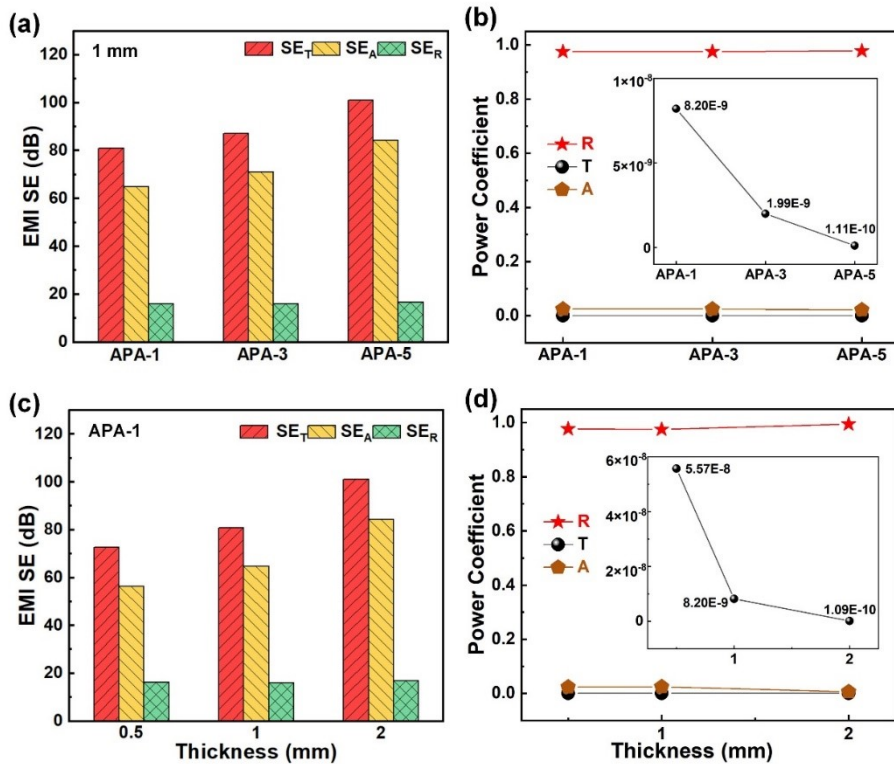


Fig. S15. (a) Average SE_T , SE_A , and SE_R and (b) average R , A , and T of the AgNW@PPy hybrid aerogels with different thicknesses of the PPy layer. (c) Average SE_T , SE_A , and SE_R and (d) average R , A , and T of the AgNW@PPy hybrid aerogels with different

thicknesses.

Table S1. Comparison of EMI shielding performance of various lightweight and porous materials

Materials	Thickness (mm)	Density (mg cm ⁻³)	EMI SE (dB)	SSE (dB cm ³ g ⁻¹)	SSE/t (dB cm ² g ⁻¹)	Ref.
AgNW@PPy hybrid aerogel	0.5		72.6	6230.2	134029.0	This work
	1	10.84	80.9	6937.1	74618.3	
	2		101.2	8679.3	46679.0	
Polymer-reinforced AgNW aerogels	2.3	4	36.4	4720	20522	1
CNF/AgNW sponge	3	41.6	81.2	1952	6506	2
V ₂ O ₅ /PANI aerogel	6	20	34.7	1662.2	2770.3	3
MXene/AgNW/melamine sponge	2	11.98	24.3	2157.6	10788	4
EPM/AgNW composites	1	61	48.5	795.4	7954	5
V ₂ O ₅ /PANI aerogel	3	40	53.6	1338.8	4462.5	6
MXene aerogel	3	5.3	34	6428	21427	7
MXene/PEDOT:PSS aerogel	5	12	59	4917	10841	8
WPU/MXene/NiFe ₂ O ₄ aerogel	2	38.2	64.7	1694	15620	9
MXene@Wood aerogel	10	108	72	667	667	10
MXene/rGO/ANF aerogel	4	62	54.8	884	2210	11
rGO/MXene aerogel	7	29	83.3	3119	4456	12
MXene/carbon aerogel	3	11.9	61.4	5115.5	17184.9	13
MXene aerogel	2	22	62.9	2846	14230	14
MXene/ANF aerogel	2.5	23.3	65.5	2847.8	11391	15
CNT/SBS foam	2	420	56	174	870	16
CNT sponge	1.8	10	54.8	5480	30444	17
rGO/CNT sponge	1.6	22.85	40	1750	10937.5	18
		6.27	67.42	10753	35843	
(Fe ₃ O ₄ @CNT)/MXene/c-ANF/PI aerogels	3	4.87	53.66	11018	36728	19
		2.47	41.79	16915	56383	
		1.62	30.45	18796	62654	
MXene/CNT aerogel	3	42	104	2476	8254	20
CNT/CMF foam	6	8.6	25.8	3688.4	6147.3	21
CNT/PU sponge	1.6	8.98	40.1	3570.6	22316	22
Graphene/AgNW aerogel	5	19	45.2	2372	4744	23
Melamine/Graphene foam	40	11	37.2	3410	845.5	24
rGO aerogel	5	8	48.6	6070	12140	25
NiCo@rGO SWNTs foam	3	13.5	75.8	5613.3	18711	26
Carbon/Graphene aerogel	1.9	74	54.6	737.8	3883	27

Carbon aerogel	4	57	40	700	1818	28
CNT/Carbon aerogel	2	34.5	84.3	2443.4	12217	29
Carbon aerogel/SnO ₂ composites	2	330	36.6	111	555	30
Ni/porous Caron	2	288	50.8	176.4	881.9	31
C-CNT/CNF aerogel	5	14 35	23.8 28	1700 800	3400 1600	32

Table S2. Comparison of Joule heating performance of various porous materials

Materials	Driven voltage (V)	Heating rate (°C s ⁻¹)	Saturation temperature (°C)	SJHE (°C cm ³ g ⁻¹ V ⁻¹)	Ref.
AgNW@PPy hybrid aerogel	1.2	390	238.5	8472	This work
Graphene aerogel	4	9.1	134	194	33
rGO aerogel	3.25	9.7	161	-	34
MXene/SA aerogel	1.2	10.2	135	860	35
Carbon aerogel/PDMS	4	0.037	137	-	36
Graphene aerogel/epoxy	5	1.2	213	-	37
Graphene foam/PDMS	2.5	0.87	78	-	38
C/rGO aerogel	8	6.7	96	1136	39
PI/MXene aerogel	10	1.57	115	170	40
cellulose/PPy/PU composite aerogels	4	2.63	173	-	41
rGO tubes aerogel/PDMS	2.5	3.5	126	-	42
MXene/ternary aerogel	8	0.75	70.3	-	43
MXene/cellulose aerogel film	9	0.58	75	-	44
CANF/CNT aerogel film	5	0.97	100.2	-	45
ANF/CNT aerogel film	10	0.32	113.5	72	46

References

- 1 Z. Zeng, W. Li, N. Wu, S. Zhao and X. Lu, *ACS Appl. Mater. Interfaces*, 2020, **12**, 38584-38592.
- 2 Y. Chen, L. Zhang, C. Mei, Y. Li, G. Duan, S. Agarwal, A. Greiner, C. Ma and S. Jiang, *ACS Appl. Mater. Interfaces*, 2020, **12**, 35513-35522.
- 3 A. Puthiyedath Narayanan, K. N. Narayanan Unni and K. Peethambharan Surendran, *Chem. Eng. J.*, 2021, **408**, 127239.
- 4 S. Wang, D. Li, W. Meng, L. Jiang and D. Fang, *J. Mater. Chem. C*, 2022, **1**, 5336-5344.
- 5 J. Wei, Z. Lin, Z. Lei, Y. Xu, Z. Zhao, T. Zhao, Y. Hu, H. Miao and R. Sun, *ACS Appl. Mater. Interfaces*, 2022, **14**, 5940-5950.
- 6 A. P. Narayanan and K. P. Surendran, *J. Mater. Chem. C*, 2022, **10**, 14754-14769.
- 7 X. Ru, H. Li, Y. Peng, Z. Fan, J. Feng, L. Gong, Z. Liu, Y. Chen and Q. Zhang, *J. Mater. Sci.-Mater. Electron.*, 2022, **33**, 4093-4103.
- 8 G. Yang, S. Wang, H. Sun, X. Yao, C. Li, Y. Li and J. Jiang, *ACS Appl. Mater. Interfaces*, 2021, **13**, 57521-57531.
- 9 Y. Wang, Q. Qi, G. Yin, W. Wang and D. Yu, *ACS Appl. Mater. Interfaces*, 2021, **13**, 21831-21843.
- 10 M. Zhu, X. Yan, H. Xu, Y. Xu and L. Kong, *Carbon*, 2021, **182**, 806-814.
- 11 F. Xie, K. Gao, L. Zhuo, F. Jia, Q. Ma and Z. Lu, *Compos. Pt. A-Appl. Sci. Manuf.*, 2022, **160**, 107049.
- 12 X. Zheng, J. Tang, P. Wang, Z. Wang, L. Zou and C. Li, *J. Colloid Inter. Sci.*, 2022, **628**, 994-1003.
- 13 S. Wu, D. Chen, W. Han, Y. Xie, G. Zhao, S. Dong, M. Tan, H. Huang, S. Xu, G. Chen, Y. Cheng and X. Zhang, *Chem. Eng. J.*, 2022, **446**, 137093.
- 14 Y. Li, Y. Chen, X. He, Z. Xiang, T. Heinze and H. Qi, *Chem. Eng. J.*, 2022, **431**, 133907.
- 15 Y. Du, J. Xu, J. Fang, Y. Zhang, X. Liu, P. Zuo and Q. Zhuang, *J. Mater. Chem. A*, 2022, **10**, 6690-6700.
- 16 D. Tian, Y. Xu, Y. Wang, Z. Lei, Z. Lin, T. Zhao, Y. Hu, R. Sun and C. Wong, *Chem. Eng. J.*, 2021, **420**, 130482.
- 17 D. Lu, Z. Mo, B. Liang, L. Yang, Z. He, H. Zhu, Z. Tang and X. Gui, *Carbon*, 2018, **133**, 457-463.
- 18 X. Zhao, L. Xu, Q. Chen, Q. Peng, M. Yang, W. Zhao, Z. Lin, F. Xu, Y. Li and X. He, *Adv. Mater. Technol.*, 2019, **4**, 1900443.
- 19 L. Zhu, R. Mo, C. Yin, W. Guo, J. Yu and J. Fan, *ACS Appl. Mater. Interfaces*, 2022, **14**, 56120-56131.
- 20 P. Sambyal, A. Iqbal, J. Hong, H. Kim, M. Kim, S. M. Hong, M. Han, Y. Gogotsi and C. M. Koo, *ACS Appl. Mater. Interfaces*, 2019, **11**, 38046-38054.
- 21 S. Zhu, S. Peng, Z. Qiang, C. Ye and M. Zhu, *Carbon*, 2022, **193**, 258-271.
- 22 X. Zhang, K. Wu, G. Zhao, H. Deng and Q. Fu, *Chem. Eng. J.*, 2022, **438**, 135659.
- 23 X. Liu, T. Chen, H. Liang, F. Qin, H. Yang and X. Guo, *RSC Adv.*, 2019, **9**, 27-33.
- 24 T. Guo, X. Chen, L. Su, C. Li, X. Huang and X. Tang, *Mater. Des.*, 2019, **182**, 108029.
- 25 S. Gupta, S. K. Sharma, D. Pradhan and N. Tai, *Compos. Pt. A-Appl. Sci. Manuf.*, 2019, **123**, 232-241.
- 26 H. Fu, L. Chen, D. Liu, Y. Zhang, Y. Cao, C. Wu, Z. Yong, Y. Yu and Q. Li, *Chem. Eng. J.*, 2023, **454**, 140324.
- 27 X. Jiang, Z. Zhao, S. Zhou, H. Zou and P. Liu, *ACS Appl. Mater. Interfaces*, 2022, **14**, 45844-45852.
- 28 L. Vazhayal, P. Wilson and K. Prabhakaran, *Chem. Eng. J.*, 2020, **381**, 122628.
- 29 Z. Zong, P. Ren, Z. Guo, J. Wang, J. Hu, Z. Chen, Y. Jin, F. Wang and F. Ren, *Carbon*, 2022, **197**,

40-51.

- 30 H. Zhao, Y. Huang, X. Wang, Y. Han, Z. Du, Y. Zheng, L. Chen and L. Jin, *Compos. Pt. A-Appl. Sci. Manuf.*, 2022, **161**, 107077.
- 31 Y. Zheng, Y. Song, T. Gao, S. Yan, H. Hu, F. Cao, Y. Duan and X. Zhang, *ACS Appl. Mater. Interfaces*, 2020, **12**, 40802-40814.
- 32 O. Pitkänen, J. Tolvanen, I. Szenti, Á. Kukovecz, J. Hannu, H. Jantunen and K. Kordas, *ACS Appl. Mater. Interfaces*, 2019, **11**, 19331-19338.
- 33 L. Feng, P. Wei, Q. Song, J. Zhang, Q. Fu, X. Jia, J. Yang, D. Shao, Y. Li, S. Wang, X. Qiang and H. Song, *ACS Nano*, 2022, **16**, 17049-17061.
- 34 D. Xia, P. Huang, H. Li and C. N. Rubio, *Chem. Commun.*, 2020, **56**, 14393-14396.
- 35 C. Qi, X. Wu, J. Liu, X. Luo, H. Zhang and Z. Yu, *J. Mater. Sci. Technol.*, 2023, **135**, 213-220.
- 36 Y. Sun, D. Li, J. U. Kim, B. Li, S. Cho, T. Kim, J. Nam, L. Ci and J. Suhr, *Carbon*, 2021, **171**, 758-767.
- 37 P. Yang, S. Ghosh, T. Xia, J. Wang, M. A. Bissett, I. A. Kinloch and S. Barg, *Compos. Sci. Technol.*, 2022, **218**, 109199.
- 38 J. Bustillos, C. Zhang, B. Boesl and A. Agarwal, *ACS Appl. Mater. Interfaces*, 2018, **10**, 5022-5029.
- 39 T. Bai, Y. Guo, D. Wang, H. Liu, G. Song, Y. Wang, Z. Guo, C. Liu and C. Shen, *J. Mater. Chem. A*, 2021, **9**, 5566-5577.
- 40 Y. Zhao, J. Chen, X. Lai, H. Li, X. Zeng, C. Jiang, Q. Zeng, K. Li, Z. Wu and Y. Qiu, *Compos. Pt. A-Appl. Sci. Manuf.*, 2022, **163**, 107210.
- 41 Y. Wang, L. Chen, H. Cheng, B. Wang, X. Feng, Z. Mao and X. Sui, *Chem. Eng. J.*, 2020, **402**, 126222.
- 42 J. Chen, B. Shen, X. Jia, Y. Liu and W. Zheng, *Mater. Today Phys.*, 2022, **24**, 100695.
- 43 C. Cai, Z. Wei, Y. Huang and Y. Fu, *Chem. Eng. J.*, 2021, **421**, 127772.
- 44 W. Xin, M. Ma and F. Chen, *ACS Appl. Nano Mater.*, 2021, **4**, 7234-7243.
- 45 C. Fu, Z. Sheng and X. Zhang, *ACS Nano*, 2022, **16**, 9378-9388.
- 46 P. Hu, J. Lyu, C. Fu, W. Gong, J. Liao, W. Lu, Y. Chen and X. Zhang, *ACS Nano*, 2020, **14**, 688-697.